Computationally Efficient Estimation of PWM-Induced Iron Loss of PMSM Using Deep Transfer Learning

Soo-Hwan Park[1], Ki-O Kim[2], and Myung-Seop Lim[2]

[1]Department of Mechanical, Robotics and Energy Engineering, Dongguk University, Seoul 04620, Republic of Korea
[2]Department of Automotive Engineering, Hanyang University, Seoul 04763, Republic of Korea

As the demand for increasing the efficiency of traction motors for increasing the mileage of electric vehicles, it is necessary to accurately estimate the efficiency of traction motors at the early design stage. Since the iron loss of the traction motor is highly affected by the pulse width modulation (PWM) frequency, the PWM current should be considered when designing the motor. However, it is difficult in considering the PWM current at the early design stage because of its high computation cost due to the small time step for representing the high-frequency harmonics. Therefore, we propose a method to reduce the computation cost for the calculation of PWM-induced iron loss using deep transfer learning (DTL) even with a small amount of data. The proposed method can be achieved by training a deep neural network (DNN) that can predict PWM-induced iron loss accurately using a large amount of sinusoidal current-based iron loss and a small amount of PWM-induced iron loss. As a result, the PWM current can be practically considered in the design stage of the traction motor because the computation cost can be decreased by using the proposed method.

***Index Terms*— Deep neural network (DNN), iron loss, permanent magnet synchronous motor (PMSM), pulse width modulation (PWM), transfer learning.**

I. Introduction

ELECTRIFICATION is an inevitable trend in the automotive industry because of environment regulation [1]. As a result, battery electric vehicles (BEVs) have been becoming the mainstream of electrification, and the value of BEVs is highly dependent on the all-electric range (AER) of BEVs. In order to increase the AER of BEVs, high efficiency and high voltage system are required for traction systems where permanent magnet synchronous motors (PMSMs) are generally used [2].

Since the efficiency of the traction motor is directly related to the electromagnetic loss, it is important to accurately calculate the electromagnetic loss considering the actual driving conditions in the design stage. In general, high-speed and low-torque operating points have a major impact on AER, so the efficiency of the traction motor is highly dependent on the iron loss [3], [4]. However, the pulse width modulation (PWM) current affects the iron loss of the traction motor due to its high-frequency terms [5]. Therefore, if the traction motor is designed based on the sinusoidal current, without considering the PWM current, there will be an error between the calculated efficiency and measured efficiency because of the effect of PWM harmonics. In order to calculate the iron loss due to the PWM current, it is necessary to calculate the magnetic flux density in the ferromagnetic materials by the PWM current. Zhao et al. [6] proposed an analytical method for calculating minor loops in non-oriented steel sheets by PWM current. As a result, it was possible to separate the total iron loss into loss due to major loop and minor loop. However, in order to calculate PWM-induced iron loss accurately, electromagnetic finite element analysis (FEA) with PWM current is necessary rather than the analytical method. Yamazaki and Seto [7] investigated the iron loss of PMSMs according to the driving condition and segregated iron loss into components by fundamental wave and PWM carriers. However, it requires high computation cost because the electromagnetic FEA should be solved with a small time step to consider the high-frequency components in PWM current [8].

In order to reduce the computation cost for calculating PWM-induced iron loss, we propose a computationally efficient estimation process of PWM-induced iron loss using deep transfer learning (DTL). The method can be achieved by using a large amount of sinusoidal current-based iron loss data with low computation cost and a small amount of PWM-induced iron loss data with high computation cost [9]. The computational cost of calculating the PWM current-considered efficiency of the main driving points due to geometry changes is very high, but the proposed method can dramatically reduce the computational cost of calculating the PWM current-considered efficiency.

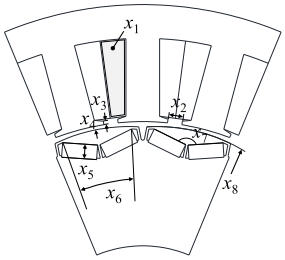

Design variables		Unit	LB	UB
x_1	Slot area	mm^2	75.0	100.0
x_2	Length of slot open	mm	1.0	4.0
x_3	Thickness of tooth tip	mm	0.5	1.2
x_4	Split ratio	-	0.65	0.75
x_5	Thickness of PM	mm	2.0	3.5
x_6	Pole arc	deg.	7.5	9.0
x_7	PM angle	deg.	38.0	85.0
x_8	Length of eccentricity	mm	9.8	33.5

Fig. 1. Geometry and design variables of 16-poles and 24-slots PMSM.

Manuscript received 25 March 2023; revised 17 July 2023; accepted 4 August 2023. Date of publication 14 August 2023; date of current version 24 October 2023. Corresponding author: M.-S. Lim (e-mail: myungseop@hanyang.ac.kr).

Color versions of one or more figures in this article are available at https://doi.org/10.1109/TMAG.2023.3304981.

Digital Object Identifier 10.1109/TMAG.2023.3304981

TABLE I
SPECIFICATIONS OF TARGET PMSM

Item	Unit	Value
Number of poles	-	16
Number of slots	-	24
Nominal battery voltage	V	144
Max. output power	kW	14.5
Peak torque	Nm	45
Max. speed	rpm	7,000
Max. current density	A_{rms}/mm^2	15.0
Switching frequency	kHz	12
Operating temperature	°C	50

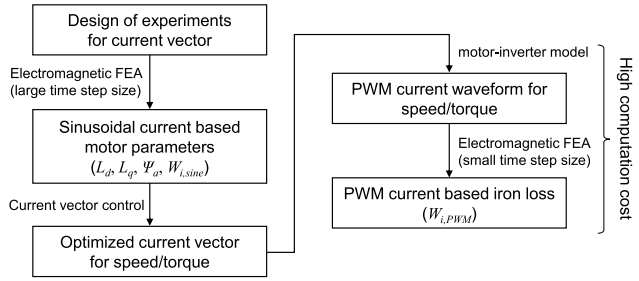

Fig. 2. Process for calculating PWM-induced iron loss.

II. CALCULATION OF PWM-INDUCED IRON LOSS

In this article, 16-pole and 24-slot PMSM is used to verify the effect of PWM harmonics on iron loss. Fig. 1 shows the geometry of 16-pole and 24-slot PMSM, and the design variables concerned with magnetic saturation and effect on the iron loss are selected for analysis of the PWM-induced iron loss of the PMSM. The detailed specifications are listed in Table I.

Since the harmonic components of PWM current vary according to the amplitude, phase, and frequency of the reference voltage, the current waveform varies according to the electromagnetic torque and rotational speed of the motor. The PWM-induced iron loss can be calculated according to the procedure shown in Fig. 2. In order to calculate the PWM current waveform according to the drive conditions, it is necessary to calculate the sinusoidal current-based motor parameters according to the current vector and rotational speed because d- and q-axis current reference should be derived to input the values to the controller. Then, the current vector control is performed to calculate the characteristics of PMSMs according to the torque and speed as shown in Fig. 3(a). After that, the PWM current can be derived using MATLAB/Simulink-based motor-inverter model.

Since the reference voltage is limited by the dc link voltage in the inverter model, the PWM current is calculated in a limited region and the region depends on the motor parameters and rotational speed. In order to reduce the computation cost for deriving PWM-induced iron loss, the PWM currents are derived only at the optimized current vector addressed with torque-speed using the sinusoidal current-based motor parameter as shown in Fig. 3(b). Then, it is possible to calculate the iron loss considering PWM current waveform

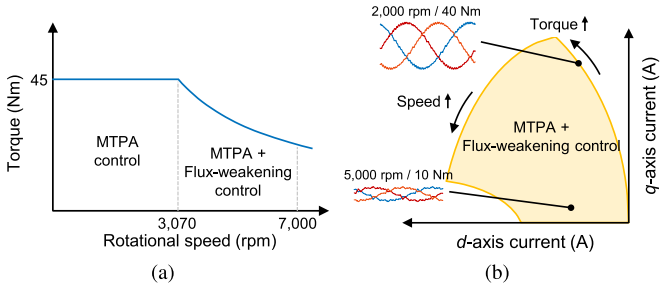

Fig. 3. Torque and speed characteristics and current waveform for each operating point of the analysis model. (a) Torque and speed curve. (b) Optimized current vector and derived PWM current waveform for each speed and torque.

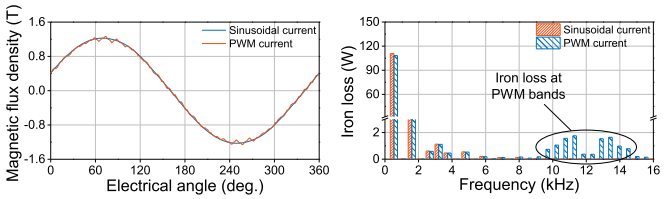

Fig. 4. Comparison of magnetic flux density for stator tooth and iron loss versus frequency under the sinusoidal current and PWM current excitation at 4000 rpm and 10 Nm. (a) Magnetic flux density at stator tooth. (b) Iron loss versus frequency.

by applying the PWM current to the electromagnetic FEA as follows:

$$W_i = \sum_{n=1}\left(V_n \sum_{m=1} W_{i,m}^n\left(B_m^n,\, f_m\right)\right) \tag{1}$$

where W_i and $W_{i,m}^n$ are the total iron loss and iron loss density per nth element and mth harmonic, respectively; B_n^m and f_m are magnetic flux density and frequency, respectively; and V_n is the volume of nth element. Fig. 4(a) and (b) shows the comparison of the magnetic flux density at stator tooth in the radial direction and iron loss versus frequency under the sinusoidal current and PWM current excitation. It can be seen that the harmonic magnetic flux density in the stator and rotor core is generated by the PWM current, and thus the additional iron loss is also generated as shown in figures. Fig. 5(a) and (b) shows the analyzed iron loss and efficiency depending on whether the PWM current is considered according to the torque and speed. It can be seen that the PWM-induced iron loss is larger than that of the sinusoidal current-induced iron loss because of additional iron loss near in PWM frequency band. As a result, the efficiency of PMSMs is highly affected by the PWM current. Although it is possible to calculate the accurate efficiency by considering the PWM current, it requires high computation cost in that an additional electromagnetic FEA should be performed with a small time step to consider the PWM frequency.

III. DTL-BASED ESTIMATION OF PWM-INDUCED IRON LOSS

A. Principle of DTL

Deep neural networks (DNNs) are generally used as a curve fitting tool in the optimization of electric machines [10]. The most effective way to improve the performance of DNNs

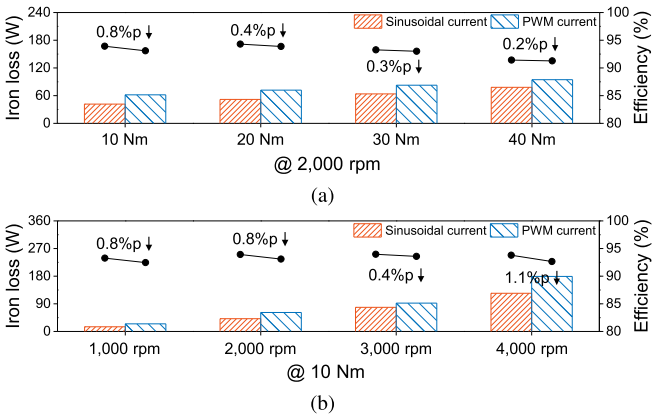

Fig. 5. Comparison between iron loss and efficiency whether the PWM current is considered according to (a) electromagnetic torque and (b) rotational speed.

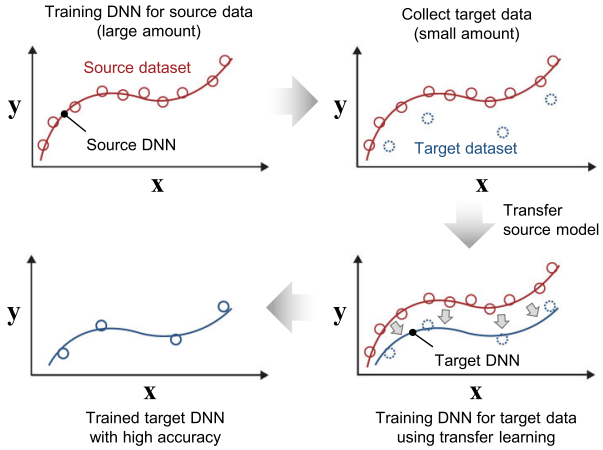

Fig. 6. Effect of DTL with a large amount of source data and a small amount of target data.

is to increase the amount of data. However, it is difficult to increase the amount of data when the required cost for labeling is high such as analyzing the iron loss with PWM current. DTL is a method that can effectively train DNN even when we have a small amount of data. The principle of DTL is as shown in Fig. 6. DTL is a learning technique that takes domain knowledge of a pre-trained model for the source dataset and utilized it to train a new neural network for the target dataset [9]. In other words, the weights of the pre-trained DNN, w', are used as the initial value of the weights of the target DNN, and the transferred weights are re-optimized to secure the transferred knowledge from the source DNN as follows:

$$\min_{w} \mathcal{L}(w) = \frac{1}{n}\sum_{i=1}^{n}\left(y_i - \hat{y}_i\right)^2 \tag{2}$$

where $\mathcal{L}$ is the loss function; n is the number of target datasets; y_i and $\hat{y}_i$ are ground truth and predicted value through the neural network, respectively.

B. Training Process of DNN for Predicting PWM-Induced Iron Loss

In this article, a surrogate model of PWM-induced iron loss is modeled using DTL to predict the efficiency of PMSM

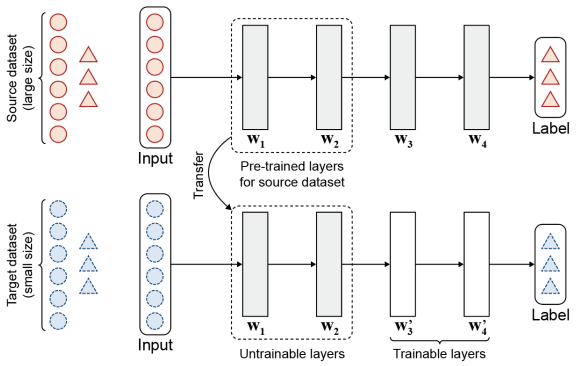

Fig. 7. Process for training the target DNN using DTL using pre-trained source DNN.

according to the geometry variation. Fig. 7 shows the process of training DNN for predicting PWM-induced iron loss using DTL. DTL is performed by setting PWM-induced iron loss as the target dataset due to the high computation cost of data acquisition, and sinusoidal current-based iron loss as the source dataset due to its similar trend with PWM-induced iron loss and low computation cost. Since the design variables are concerned with magnetic saturation, the input layer of the DNN consists of 11 nodes, which includes the design variables, d- and q-axis current, and rotational speed, and the output layer consists of one node to predict iron loss.

The detailed process of obtaining the dataset is as follows. First, the design of experiments is performed on the design variables. The design points are selected using Latin hypercube sampling (LHS), and the peak current is calculated using the current density and slot area determined by the geometry of the PMSM as follows:

$$i_{pk} = J_{\max}\frac{A_{\text{slot}} \cdot k_{\text{Cu}}}{N_c} \tag{3}$$

where i_{pk} and $J_{\max}$ are the peak current and maximum current density, respectively; A_{slot} and k_{Cu} are the slot area and effective slot fill factor without considering insulation of copper wire; N_c is the number of conductors per slot. Then, d- and q-axis current and rotational speed can be sub-sampled based on the maximum current at each design point, and the motor parameters consisting of d- and q-axis inductance, flux-linkage, and iron loss per design point are analyzed with the sinusoidal current. Thus, the source dataset can be built consisting of the design variables, d- and q-axis current, and the rotational speed and corresponding sinusoidal current-based iron loss. Meanwhile, LHS-based sub-sampling according to the design point is performed to optimize the current vector for PWM current-based iron loss analysis within the maximum torque and power of the PMSM. Finally, the PWM-induced iron loss can be analyzed and the target dataset is constructed with the design variables, d- and q-axis current, and rotational speed. Since the PWM-induced iron loss requires high computation cost, the number of target datasets is 8.6% of the number of source datasets.

After that, the source and target DNNs are trained with source and target datasets using DTL. The architecture of DNN is set as multi-layer perceptron (MLP), and the detailed training conditions and a number of datasets are shown in

TABLE II
HYPERPARAMETER SETTING OF DNN AND NUMBER OF DATASETS

Input features	Design variables of PMSM, $i_{d,q}$, ω_m	
Output features	$W_{i,1st}$	$W_{i,PWM}$
Number of layers	4	
Number of units	256	
Learning rate	1e-5	
Activation function	ReLU	
Optimizer	Adam	
Loss function	Mean squared error	
Size of mini-batch	32	
Number of dataset	63,000 (Source)	3,640 (Target)

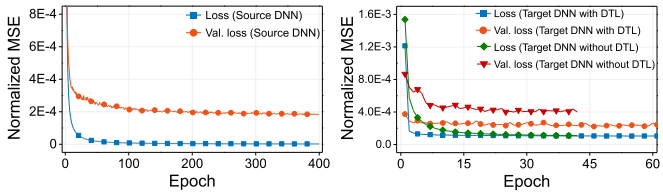

(a) (b)

Fig. 8. Training and validation loss for building DNN to predict. (a) Sinusoidal current-based iron loss. (b) PWM-induced iron loss.

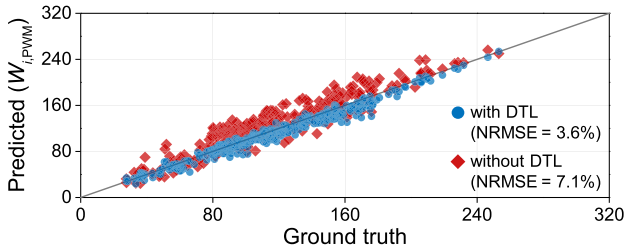

Fig. 9. Comparison of ground truth and predicted result for PWM-induced iron loss with or without using DTL.

Table II. As a result of hyperparameter tuning, the number of hidden layers, units, and learning rate were selected as 4, 256, and 1e-5, respectively. In order to avoid overfitting the source and target dataset were divided into training, validation, and test sets with a ratio of 8:1:1. In order to utilize the domain knowledge of the source DNN that has a similar distribution to the target dataset, the layers of the target DNN except for several top layers are transferred from the pre-trained layers of source DNN. Then, the target DNN is additionally trained using the target dataset.

Fig. 8(a) and (b) shows the learning curves of source and target DNN for predicting sinusoidal current-based iron loss and PWM-induced iron loss. In order to verify the effectiveness of DTL, the results with or without using DTL are compared. It can be seen that the training and validation loss of source DNN converged at low values without overfitting because the number of source datasets is large enough. However, it can be seen that the loss quickly converged to a relatively high value as a result of training the target DNN without DTL. This is because the number of training data is very small and overfitting to the validation set occurred at an early in the training process. On the other hand, it can be seen that

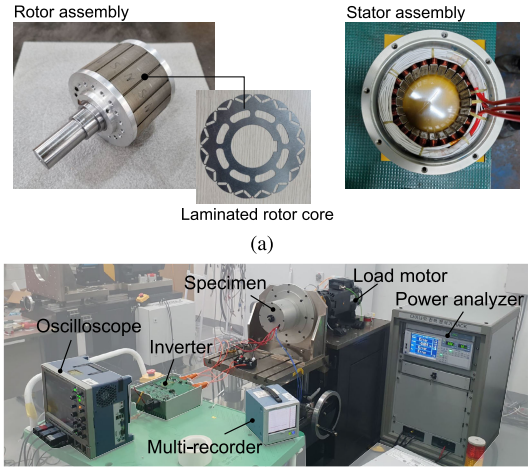

(a) (b)

Fig. 10. Fabricated specimen consists of (a) stator and rotor for verifying PWM-induced iron loss and (b) experimental setup for a load test.

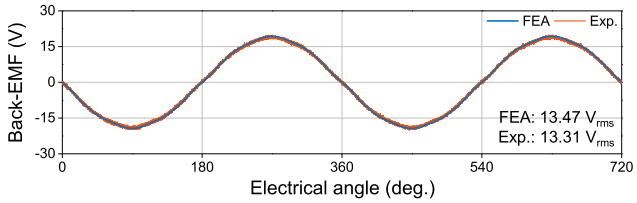

Fig. 11. Comparison between measured and calculated no-load Back EMF of the specimen.

the loss converged to a low value through sufficient training by using DTL. Fig. 9 shows the comparison of ground truth and prediction for PWM-induced iron loss with or without using DTL. As a result of using DTL, it can be seen that the regression performance on the test dataset was highly well evaluated, where the normalized root mean squared error (NRMSE) is 3.6%, and as a result of the training from scratch without using DTL, it can be seen that the performance was degraded, where NRMSE is 7.1%, due to the target DNN was overfitted to the training dataset. Consequently, the prediction of PWM-induced iron loss can be conducted with high accuracy even with a small amount of dataset by using DTL.

IV. EXPERIMENTAL VERIFICATION

In order to verify the predicted results of PWM-induced iron loss, a specimen located within the design variable range was fabricated and a load test was conducted. Fig. 10(a) and (b) shows the fabricated specimen and experimental setup. Before conducting the load test, the measured and simulated no-load back-electromotive force (Back EMF) were compared to verify the magnetic circuit of the specimen as shown in Fig. 11. The measurement was performed at room temperature and the no-load Back EMF was measured at 1000 rpm. It can be seen that the error was 1.5% so the results from the electromagnetic FEA have consistency with the experiment.

The load test was performed at 2100 rpm, 12.5 Nm, and 4100 rpm, 12.5 Nm to verify the PWM-induced iron loss predicted using DTL. Since the iron loss is caused by the

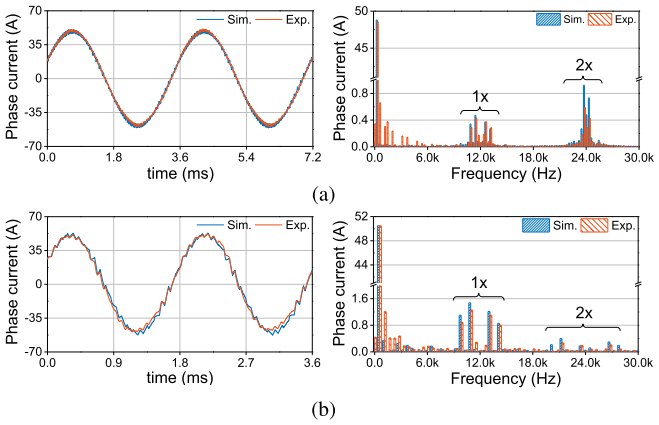

Fig. 12. Comparison of measured and simulated PWM current at each operating point (a) 2100 rpm, 12.5 Nm and (b) 4100 rpm, 12.5 Nm.

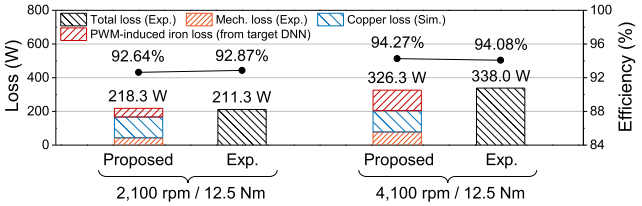

Fig. 13. Comparison of loss and efficiency at each operating point.

magnetic flux density fluctuations in the stator and rotor core, the iron loss is caused by the fundamental wave of the current waveform and the harmonics near PWM bands. Since the consistency between experiments and FEM analysis of sinusoidal current-based and PWM current-based iron loss was verified by [11], the PWM-induced iron loss was verified in this article. First, the PWM current was compared to verify the consistency of the data used for training DNN as shown in Fig. 12(a) and (b). Since the PWM voltage was controlled at a switching frequency of 12 kHz, a harmonic band was observed around twice the switching frequency, and the simulation results also showed the same result. In addition, the small error of the amplitude of the harmonic current refers that the error of the motor parameters used in the simulation was also small. Fig. 13 shows the result of comparing the loss and efficiency considering PWM-induced iron loss predicted through the proposed method and the measured efficiency. The mechanical loss and dc copper loss were considered in the calculation of efficiency, but permanent magnet eddy current loss was not considered. As a result of using DTL, the error of total loss between the experiment and predicted result using DTL was 3.3% and 3.5%, respectively, and 0.2%p and 0.2%p for efficiency, respectively. It can be seen that the efficiency was predicted at a reasonable level so that the proposed method can be widely used for optimizing the efficiency of PMSM because the efficiency considering the PWM-induced iron loss can be predicted with a very small computation cost.

V. Conclusion

When calculating the PWM-induced iron loss, high computation cost is required because the process for deriving the PWM current waveform and short time step electromagnetic FEA are involved. Therefore, a computationally efficient method for the prediction of PWM-induced iron loss of PMSM is proposed using DTL in this article. First, the difference in PWM current waveforms according to the operating point and the effect of PWM-induced iron loss on the efficiency of PMSM was analyzed. Then, the principle of DTL for training a surrogate model that predicts PWM-induced iron loss with high accuracy using a large amount of sinusoidal current-based iron loss and a small amount of PWM-induced iron loss was described. The performance of the surrogate model was verified by applying the proposed method to a 16-pole and 24-slot PMSM. Finally, a specimen was fabricated for experimental verification, and simulation and experiment results of PWM current and efficiency were compared.

Acknowledgment

This work was supported by the National Research Foundation of Korea (NRF) grant funded by the Korea Government (MSIT) under Grant RS-2023-00207865.

References

[1] Y. Yang et al., "Design and comparison of interior permanent magnet motor topologies for traction applications," *IEEE Trans. Transport. Electrific.*, vol. 3, no. 1, pp. 86–97, Mar. 2017.

[2] I. Aghabali, J. Bauman, P. J. Kollmeyer, Y. Wang, B. Bilgin, and A. Emadi, "800-V electric vehicle powertrains: Review and analysis of benefits, challenges, and future trends," *IEEE Trans. Transport. Electrific.*, vol. 7, no. 3, pp. 927–948, Sep. 2021.

[3] A. G. Sarigiannidis, M. E. Beniakar, and A. G. Kladas, "Fast adaptive evolutionary PM traction motor optimization based on electric vehicle drive cycle," *IEEE Trans. Veh. Technol.*, vol. 66, no. 7, pp. 5762–5774, Jul. 2017.

[4] S.-W. Hwang, J.-Y. Ryu, J.-W. Chin, S.-H. Park, D.-K. Kim, and M.-S. Lim, "Coupled electromagnetic-thermal analysis for predicting traction motor characteristics according to electric vehicle driving cycle," *IEEE Trans. Veh. Technol.*, vol. 70, no. 5, pp. 4262–4272, May 2021.

[5] D. Jiang and F. Wang, "Current-ripple prediction for three-phase PWM converters," *IEEE Trans. Ind. Appl.*, vol. 50, no. 1, pp. 531–538, Jan. 2014.

[6] H. Zhao, C. Ragusa, O. de la Barrière, M. Khan, C. Appino, and F. Fiorillo, "Magnetic loss versus frequency in non-oriented steel sheets and its prediction: Minor loops, PWM, and the limits of the analytical approach," *IEEE Trans. Magn.*, vol. 53, no. 11, pp. 1–4, Nov. 2017.

[7] K. Yamazaki and Y. Seto, "Iron loss analysis of interior permanent-magnet synchronous motors-variation of main loss factors due to driving condition," *IEEE Trans. Ind. Appl.*, vol. 42, no. 4, pp. 1045–1052, Aug. 2006.

[8] L. Chang, T. M. Jahns, and R. Blissenbach, "Estimation of PWM—Induced iron loss in IPM machines incorporating the impact of flux ripple waveshape and nonlinear magnetic characteristics," *IEEE Trans. Ind. Appl.*, vol. 56, no. 2, pp. 1332–1345, Mar. 2020.

[9] S.-H. Park, J.-W. Chin, K.-S. Cha, and M.-S. Lim, "Deep transfer learning-based sizing method of permanent magnet synchronous motors considering axial leakage flux," *IEEE Trans. Magn.*, vol. 58, no. 9, pp. 1–5, Sep. 2022.

[10] Y. Shimizu, S. Morimoto, M. Sanada, and Y. Inoue, "Automatic design system with generative adversarial network and convolutional neural network for optimization design of interior permanent magnet synchronous motor," *IEEE Trans. Energy Convers.*, vol. 38, no. 1, pp. 724–734, Mar. 2023.

[11] Z. Gmyrek, A. Boglietti, and A. Cavagnino, "Estimation of iron losses in induction motors: Calculation method, results, and analysis," *IEEE Trans. Ind. Electron.*, vol. 57, no. 1, pp. 161–171, Jan. 2010.